Published in final edited form as:
Oncogene. 2009 February 5; 28(5): 638–650. doi:10.1038/onc.2008.418.

ILEI requires oncogenic Ras for the epithelial to mesenchymal transition of hepatocytes and liver carcinoma progression

C Lahsnig[1], **M Mikula**[2], **M Petz**[2], **G Zulehner**[1], **D Schneller**[1], **F van Zijl**[1], **H Huber**[1], **A Csiszar**[2], **H Beug**[2], and **W Mikulits**[1]

[1]Division: Institute of Cancer Research, Department of Medicine I, Medical University of Vienna, Borschke-Gasse 8a, Vienna, Austria

[2]Research Institute of Molecular Pathology, Dr Bohr-Gasse 7, Vienna, Austria

Abstract

In human hepatocellular carcinoma (HCC), epithelial to mesenchymal transition (EMT) correlates with aggressiveness of tumors and poor survival. We employed a model of EMT based on immortalized $p19^{ARF}$ null hepatocytes (MIM), which display tumor growth upon expression of oncogenic Ras and undergo EMT through the synergism of Ras and transforming growth factor (TGF)-β. Here, we show that the interleukin-related protein interleukin-like EMT inducer (ILEI), a novel EMT-, tumor- and metastasis-inducing protein, cooperates with oncogenic Ras to cause TGF-β-independent EMT. Ras-transformed MIM hepatocytes overexpressing ILEI showed cytoplasmic E-cadherin, loss of ZO-1 and induction of α-smooth muscle actin as well as platelet-derived growth factor (PDGF)/PDGF-R isoforms. As shown by dominant-negative PDGF-R expression in these cells, ILEI-induced PDGF signaling was required for enhanced cell migration, nuclear accumulation of β-catenin, nuclear pY-Stat3 and accelerated growth of lung metastases. In MIM hepatocytes expressing the Ras mutant V12-C40, ILEI collaborated with PI3K signaling resulting in tumor formation without EMT. Clinically, human HCC samples showed granular or cytoplasmic localization of ILEI correlating with well and poorly differentiated tumors, respectively. In conclusion, these data indicate that ILEI requires cooperation with oncogenic Ras to govern hepatocellular EMT through mechanisms involving PDGF-R/β-catenin and PDGF-R/Stat3 signaling.

Keywords

hepatocyte; ILEI; epithelial to mesenchymal transition; HCC; tumor progression

Introduction

Hepatocellular carcinoma (HCC) accounts for 5.5% of all cancer cases worldwide (Kensler *et al.*, 2003). Owing to the aggressive behavior and the poor prognosis at advanced stages, HCC globally belongs to the third leading cause of cancer mortality (Bruix *et al.*, 2004). HCC arise through abnormal proliferation and dedifferentiation of hepatocytes, caused by hepatitis Bor C virus infections, dietary exposure to fungal hepatotoxins or alcohol intoxication (Thorgeirsson and Grisham, 2002). Most frequently occurring molecular

Correspondence: Professor W Mikulits, Division: Institute of Cancer Research, Department of Medicine I, Medical University of Vienna, Borschke-Gasse 8a, A-1090 Vienna, Austria. wolfgang.mikulits@meduniwien.ac.at.

Supplementary Information accompanies the paper on the Oncogene website (http://www.nature.com/onc)

Europe PMC Funders Author Manuscripts

alterations in HCC include the (i) loss of tumor suppressors involving p53, pRB, cyclins/cdks or the CDKN2A-encoded proteins $p14^{ARF}$ and $p16^{INK4a}$ (Tannapfel *et al.*, 2001; El-Serag and Rudolph, 2007), (ii) loss of the cell–cell adhesion protein E-cadherin (Kondoh *et al.*, 2001), (iii) activation of oncoproteins-for example, receptor tyrosine kinases-causing strongly enhanced Erk/mitogen-activated protein kinase (MAPK) and PI3K signaling (Breuhahn *et al.*, 2006), (iv) nuclear accumulation of Wnt/β-catenin (Lee *et al.*, 2006a) and (v) aberrant regulation and secretion of cytokines such as transforming growth factor (TGF)-β (Rossmanith and Schulte-Hermann, 2001). Although the knowledge of mechanisms involved in HCC is rapidly growing (Herath *et al.*, 2006), the molecular pathogenesis of HCC is still poorly understood.

Epithelial to mesenchymal transition (EMT) is a developmental event increasingly recognized as a central process during cancer progression and metastasis (Grunert *et al.*, 2003; Thiery and Sleeman, 2006; Hugo *et al.*, 2007). Multiple molecular mechanisms have been identified to induce EMT (Huber *et al.*, 2005), including TGF-β/TGF-βRI signaling, which collaborates with other signaling effectors to disintegrate tight junctions and E-cadherin/β-catenin complexes at cell–cell contacts (Thiery and Sleeman, 2006; Pardali and Moustakas, 2007). In human HCC, Laminin-5 and TGF-β1 have been described to cooperatively induce EMT at the invasive front of metastatic tumors (Giannelli *et al.*, 2005). In addition, signal transducer and activator of transcription (Stat)5b collaborates with the hepatitis B oncoprotein HBX to cause EMT and invasiveness of HCC (Lee *et al.*, 2006b).

To study EMT in hepatocytes, we employed Met murine hepatocytes immortalized by transgenic expression of cyto-Met (Gotzmann *et al.*, 2002) or an unique model of hepatocytes derived from $p19^{ARF}$ null mice. Although wild-type mouse hepatocytes cannot be expanded because of mitotic inactivity and rapid dedifferentiation, $p19^{ARF}$-deficient MIM1-4 hepatocytes proliferate and show characteristics of normal hepatocytes such as expression of albumin and the ability to restore the liver after injury (Mikula *et al.*, 2004). In both Met murine hepatocytes and MIM1-4 hepatocytes, the synergistic action of oncogenic Ras and TGF-β signaling induces EMT resulting in a highly malignant, invasive phenotype (Gotzmann *et al.*, 2002, 2006). Studies of EMT in MIM hepatocytes by employing Ras subeffector mutants revealed that Erk/MAPK signaling is sufficient to induce and maintain hepatocellular EMT in cooperation with TGF-β. On the contrary, the selective activation of PI3K signaling by expression of V12-C40-Ras showed lack of EMT and tumor formation (Fischer *et al.*, 2005). Furthermore, the molecular collaboration between oncogenic Ras and TGF-β signaling causes the upregulation of platelet-derived growth factor (PDGF)/PDGF-R components, which are responsible for the nuclear accumulation of β-catenin, the latter representing a hallmark of human HCC (Fischer *et al.*, 2007).

Recently, expression profiling of polysome-bound mRNA revealed interleukin-like EMT inducer (ILEI) as a novel regulator of EMT (Waerner *et al.*, 2006). In the mammary EpH4/EpRas model, overexpression of ILEI causes EMT, tumor growth and metastasis upon tail vein injection. Moreover, RNAi-mediated suppression of ILEI prevents EMT and metastasis in various murine and human cellular models (Waerner *et al.*, 2006), suggesting that ILEI is both necessary and sufficient for these processes. Importantly, ILEI localization in cytoplasmic particles was identified as an independent parameter predictive for metastasis development and shortened survival of breast cancer patients. Cytoplasmic ILEI localization was also observed in nuclear β-catenin-positive tumor cells, which have undergone EMT at the invasive front of colon carcinomas (Waerner *et al.*, 2006).

In this study, we analysed the function of ILEI in MIM hepatocytes and determined how ILEI affects EMT and liver carcinogenesis. We found that ILEI required the cooperation with oncogenic Ras to induce and maintain EMT of hepatocytes in a TGF-β-independent

Europe PMC Funders Author Manuscripts

fashion. Ras/ILEI expressing MIM hepatocytes exhibited upregulation of PDGF/PDGF-R associated with Stat3 activation and nuclear accumulation of β-catenin. In human HCC samples, cytoplasmic localization of ILEI correlated with poor differentiation and prognosis as recently observed in breast cancer patients.

Results

ILEI is expressed and differentially localized during TGF-β-dependent EMT of hepatocytes

First, we analysed the expression of endogenous ILEI by immunohistochemistry in experimental tumors derived from epithelial hepatocytes expressing oncogenic Ras (all MIM-R-green fluorescent protein (GFP)) and from the same cells after EMT upon long-term treatment with TGF-β1, resulting in fibroblastoid MIM-RT cells (Fischer *et al.*, 2007). ILEI was hardly detectable in normal liver, whereas prominent expression of ILEI was observed in orthotopic tumors formed by MIM-R-GFP and MIM-RT cells (Figure 1a). Moderatly differentiated tumors, generated by epithelial MIM-R-GFP cells, showed granular staining of ILEI (Figure 1a). In contrast, poorly differentiated tumors generated from fibroblastoid MIM-RT cells exhibited cytoplasmic staining of ILEI (Figure 1a). Furthermore, pulmonary metastatic colonies of fibroblastoid MIM-RT cells after tail vein injection revealed a mixed cytoplasmic and granular localization of ILEI, suggesting a partial reversal of EMT in metastatic nodules. From these data we concluded that ILEI is expressed in mouse hepato-cellular carcinoma but not in normal liver, and is subject to differential localization during EMT and cancer progression.

ILEI collaborates with oncogenic Ras to induce and maintain EMT of hepatocytes

We assessed the role of ILEI in hepatocellular EMT by its stable overexpression in immortalized MIM1-4 hepatocytes, either alone (MIM1-4-ILEI), together with oncogenic Ras (MIM-R-ILEI) or in cooperation with the PI3K-hyperactivating Ras mutant V12-C40 (MIM-C40-ILEI). Overexpression of total ILEI was verified by western blot analysis, showing a 2-4-fold increase in all cell types (Figure 1b).

ILEI expression on its own or together with V12-C40-Ras did not result in significant morphological changes in culture (Figure 2), neither in sparse nor dense monolayers (Supplementary Figure S1a). However, ILEI overexpression in oncogenic Ras-transformed MIM-R-GFP hepatocytes induced a shift from an epithelial to a fibroblastoid morphology, regardless of cell density (Figure 2 and Supplementary Figure S1b).

In line with their epithelial morphology, MIM1-4-ILEI hepatocytes showed plasma membrane localization of the epithelial markers ZO-1, E-cadherin and β-catenin similar to MIM1-4-GFP control cells, suggesting intact epithelial cell-cell contacts (Supplementary Figure S2a). Furthermore, ILEI did neither affect β-actin localization nor elevate the mesenchymal marker α-smooth muscle actin (α-SMA) expression (Supplementary Figure S2b). In addition, ILEI failed to induce TGF-β/Smad signaling as Smad2/Smad3 were entirely cytoplasmic in both MIM1-4-GFP and MIM1-4-ILEI cells. Yet, MIM1-4-ILEI cells showed a weak increase of active, nondestructible β-catenin in nuclei (Supplementary Figure S2a).

Coexpression of ILEI and V12-C40-Ras in MIM1-4 cells (MIM-C40-ILEI) resulted in a similar marker expression as in MIM1-4-ILEI hepatocytes, that is, plasma membrane localization of ZO-1, E-cadherin, β-catenin and β-actin (Figure 2). MIM-C40-ILEI cells, however, displayed elevated nuclear accumulation of β-catenin as compared with MIM1-4-GFP cells as well as enhanced expression of α-SMA (Supplementary Figure S3). In contrast, ILEI plus oncogenic Ras in MIM-R-ILEI cells led to a stable EMT phenotype resembling the one observed in MIM-RT cells (Fischer *et al.*, 2005). MIM-R-ILEI cells

showed a fibroblastoid morphology, strong reduction of ZO-1, cytoplasmic redistribution of E-cadherin and relocalization of β-actin from the plasma membrane to stress fibers (Figure 2). Furthermore, MIM-R-ILEI cells showed strong nuclear accumulation of β-catenin (Figure 2) and enhanced expression of α-SMA (Supplementary Figure S3). In addition, ILEI induced a partial shift of nuclear to cytoplasmic Smad2/Smad3 localization in both MIM-C40-GFP and MIM-R-GFP cells (Supplementary Figure S3), suggesting that TGF-β/Smad signaling is inhibited rather than activated. This independence of ILEI action from TGF-βR signaling was confirmed by (i) the reduction of secreted TGF-β levels by ILEI in all cell types (Supplementary Figure S4), (ii) the inability of the TGFβ-RI/II kinase inhibitor LY02109761 (Lacher *et al.*, 2006) to reverse MIM-R-ILEI cells to an epithelial phenotype (data not shown) and (iii) the absence of reporter activities in MIM-R-ILEI cells after transfection of Smad2- or Smad3-dependent luciferase constructs (data not shown). These results show that ILEI requires oncogenic Ras, but not TGF-β/Smad signaling to induce and maintain hepatocellular EMT *in vitro*.

ILEI stimulates upregulation of PDGF-C/PDGF-Rβ and enhances proliferation and migration in oncogenic Ras-expressing MIM-R-GFP hepatocytes

Next, we analysed the expression of several EMT-specific genes in MIM-R-GFP, MIM-R-ILEI and MIM-RT cells. Proteins strongly reduced (E-cadherin) or elevated (MMP-9) in MIM-RT cells showed weaker down- or upregulation in MIM-R-ILEI cells, respectively (Figure 3a). With the exception of Slug, the EMT-inducing transcription factors Twist (Yang *et al.*, 2004) and ZEB1/Δ-EF1 (Eger *et al.*, 2005) were induced in MIM-R-ILEI cells, but surprisingly not in MIM-RT cells (Figure 3a). As an autocrine loop of PDGF/PDGF-R is essential for hepatocellular EMT (Gotzmann *et al.*, 2006) and the EMT in EpH4/EpRas cells (Jechlinger *et al.*, 2006), we focused on the effect of exogenous ILEI on the expression of different PDGF and PDGF-R isoforms in these cells. Interestingly, ILEI induced a strong increase of PDGF-C in MIM1-4-ILEI, MIM-C40-ILEI or MIM-R-GFP-ILEI cells (Figure 3b). In contrast, the cooperation of ILEI and oncogenic Ras in MIM-R-ILEI cells was necessary to induce PDGF-Rβ expression, which was very low in MIM-R-GFP cells and undetectable in MIM1-4-GFP and MIM-C40-GFP hepatocytes expressing or lacking exogenous ILEI. These findings suggest an involvement of an autocrine PDGF-C/PDGF-Rβ loop in ILEI-induced EMT of MIM-R-GFP hepatocytes.

We further assessed the effect of exogenous ILEI and PDGF/PDGF-R signaling on the proliferation of parental MIM1-4-GFP and MIM-R-GFP hepatocytes. MIM1-4-GFP and MIM-R-GFP cells proliferated with doubling times of 23 and 15 h, respectively (Figures 4a and b), whereas exogenous ILEI expression hardly altered doubling times (MIM1-4-ILEI, 22 h; MIM-R-ILEI, 15 h). Expression of a dominant-negative (dn) PDGF-R mutant, however, strongly inhibited proliferation of MIM-R-ILEI cells (doubling time of MIM-R-ILEI-dnP cells, 31 h; Figure 4a). Control MIM-R-GFP-dnP hepatocytes expressing the dn PDGF-R showed proliferation kinetics comparable to MIM-R-GFP hepatocytes as described recently (data not shown; (Fischer *et al.*, 2007)).

In line with the TGF-β-independent function of ILEI in hepatocytes described above, MIM1-4-GFP and MIM1-4-ILEI cells underwent proliferation arrest and cell death with similar kinetics. TGF-β, however, inhibited early proliferation of MIM1-4-GFP cells (during the first 5 cell divisions) more strongly than of MIM1-4-ILEI cells (Figure 4b). Therefore, active TGF-β/Smad signaling causes growth arrest and cell death in MIM1-4 cells lacking or expressing ILEI, except that ILEI may exert early and transient protective effects on proliferation. In contrast, Ras-expressing MIM-R-ILEI and MIM-R-GFP-hepatocytes were both protected from TGF-β-dependent cell cycle arrest and cell death, showing exponential proliferation in the presence and absence of TGF-β (Figure 4c; data not shown).

Another parameter important in EMT is the migratory potential of cells as analysed by Transwell filters. Interestingly, ILEI enhanced the migration not only of MIM-R-GFP hepatocytes (as expected from their fibroblastoid phenotype) but also of MIM-C40-GFP cells (Figure 4d). This correlates with the fact that MIM-C40-ILEI but not MIM-C40-GFP cells are tumorigenic (see below). This ILEI-dependent increase in migratory activity also required autocrine PDGF/PDGF-R signaling since its blockade by dn PDGF-R in MIM-R-ILEI-dnP cells reduced migration to control levels in MIM-R-GFP cells (Figure 4d). From these data we concluded that PDGF-R signaling enhanced both cell proliferation and migration of hepatocytes that have undergone Ras/ILEI-mediated EMT.

The collaboration of ILEI with oncogenic Ras enhances tumor formation, nuclear accumulation of β-catenin and Stat3 tyrosine phosphorylation

We next investigated the tumorigenicity of ILEI-overexpressing hepatocytes and found that exogenous ILEI expression in MIM1-4-ILEI cells did not cause tumor growth (data not shown). Overexpression of ILEI in MIM-R-GFP (MIM-R-ILEI) cells, however, resulted in a 4.5-fold increase of tumor size irrespective of the absence or presence of dn PDGF-R (MIM-R-ILEI-dnP cells; Figure 5a). Tumor growth of control MIM-R-GFP-dnP hepatocytes expressing the dn PDGF-R was slightly lower as compared with MIM-R-GFP cells (data not shown; (Gotzmann *et al.*, 2006; Fischer *et al.*, 2007)). Interestingly, ILEI induced tumorigenicity of MIM-C40-GFP hepatocytes (Figure 5b), which are strictly nontumorigenic in the absence of ILEI (Figure 5b (Fischer *et al.*, 2005)). Remarkably, tumors derived from MIM-C40-ILEI cells showed a delay in tumor formation (detectable after 14 days) and a slower growth rate as compared with MIM-R-ILEI-induced tumors, but reached similar volumes and tumor weights as MIM-R-ILEI tumors (Figure 5c).

Immunohistochemical analysis of sections from epithelial MIM-R-GFP- and MIM-R-GFP-dnP-derived tumors showed that E-cadherin and β-catenin localized at cell boundaries of most tumor cells, suggesting the presence of functional cell adhesion complexes (Figure 6a). In contrast, tumors generated from MIM-R-ILEI cells showed aspects of EMT *in vivo* such as cytoplasmic E-cadherin, partial loss of plasma membrane-localized β-catenin and strong nuclear staining of β-catenin (28% of cells; Figures 6a and b). Although MIM-R-ILEI and MIM-R-ILEI-dnP-induced tumors resulted in comparable volumes (Figure 5a), intervention with PDGF-R signaling in MIM-R-ILEI-dnP tumors caused re-expression of plasma membrane-localized E-cadherin and reduced β-catenin nuclear translocation (Figure 6a). The restoration of E-cadherin expression at cell borders of MIM-R-ILEI-dnP cells was also prominent in cell culture when compared with MIM-R-ILEI cells (Supplementary Figure S5). In conclusion, ILEI in collaboration with Ras induced a similar PDGF-R-dependent EMT phenotype as observed in MIM-RT tumors, that is, weak cytoplasmic E-cadherin staining and accumulation of nuclear β-catenin generated by oncogenic Ras plus prolonged TGF-β exposure (Supplementary Figure S6; Fischer *et al.*, 2007).

PDGF-R signaling causes tyrosine phosphorylation of Stat3 (pY-Stat3) through Src activation (Garcia *et al.*, 2001). Thus, we analysed the above tumor types for pY-Stat3 and total Stat3, as well as ILEI expression. Interestingly, MIM-R-ILEI-induced tumors (cytoplasmic ILEI staining) showed intense nuclear staining for pY-Stat3 in 27% of cells, whereas only 8 and 11% of cells in MIM-R-GFP and MIM-R-GFP-dnP tumors (both granular ILEI staining) showed nuclei positive for pY-Stat3, respectively (Figures 7a and b). As expected, blockade of PDGF-R signaling in MIM-R-ILEI-dnP cells reduced pY-Stat3 expression to intermediate levels and still showed cytoplasmic ILEI staining (Figure 7a), in line with their unaltered tumorigenicity (Figure 5a). In contrast, immunohistochemical staining for total Stat3 was similar in all three cell types (Figures 7a and b). These data show that the Ras/ILEI induced upregulation of PDGF/PDGF-R isoforms causes nuclear accumulation of both activated β-catenin and pY-Stat3.

ILEI enhances the growth rate of MIM-R-GFP-derived metastatic colonies

We further asked whether ILEI overexpression enhances metastasis of MIM-R-GFP hepatocytes and whether metastasis requires PDGF-R signaling. Thus, we analysed the effect of ILEI overexpression on metastasis and its requirement for PDGF-R signaling in MIM-R-GFP cells already causing liver tumors, which metastasize to the lung. MIM-R-GFP, MIM-R-GFP-dnP, MIM-R-ILEI or MIM-R-ILEI-dnP cells were injected into the tail vein of severe combined immunodeficiency (SCID) mice and further analysed for lung colonization. Whereas the frequency of lung metastases was similar in the four groups of mice, the size of lung metastases was slightly enhanced in mice receiving MIM-R-ILEI cells but strongly reduced in those injected with MIM-R-ILEI-dnP cells (Supplementary Figure S7a and S7b). MIM-R-ILEI-dnP cells showed almost no metastases with more than 100 cells while approximately 40% of MIM-R-ILEI-derived metastases contained >100 cells (Supplementary Figure S7b). In addition, immunohistochemical staining of sections from these metastases revealed that ILEI was predominantly localized in the cytoplasm of MIM-R-GFP and MIM-R-ILEI cells, whereas MIM-R-ILEI-dnP-derived metastases showed also granular areas overlapping with nuclei (Supplementary Figure S7c). These data suggest that ILEI-induced PDGF signaling increases the growth rate of metastatic colonies from hepatocytes expressing oncogenic Ras.

Cytoplasmic localization of ILEI correlates with tumor dedifferentiation in human HCCs

Recently, it has been described that cytoplasmic expression of ILEI was strongly enhanced in metastatic breast carcinomas and tumor-host borders of invasive colon carcinomas (Waerner *et al.*, 2006). In an attempt to bridge mouse and human hepatocarcinogenesis with respect to the importance of ILEI expression and localization for HCC patient prognosis, a tissue array covering 69 human HCC samples was immunohistochemically analysed. ILEI staining intensities were distinguished between no, weak or strong staining (Figure 8a). In addition, we further discriminated between granular (G) and cytoplasmic staining (C) to evaluate the intracellular localization of ILEI (Figure 8a). The important parameter yielding a clear result was postoperative, histological grading (pG0 to pG3), which is described to predict good to bad prognosis (Edmondson and Steiner, 1954; Zhou *et al.*, 2007). Granular staining was not predictive for differentiated HCC with good prognosis. Interestingly, moderately or strongly dedifferentiated tumors (pG2–pG3 grades) were positive for strong cytoplasmic staining at a higher frequency (66%) than pG0 (28%). In contrast, weak cytoplasmic ILEI staining predicted pG0 (72%) rather than dedifferentiated tumors (pG2–pG3; 34%). These data suggest that strong cytoplasmic ILEI staining can predict poor differentiation and prognosis of human HCC.

Discussion

We used $p19^{ARF}$-deficient hepatocytes as a physiologically relevant model to analyse the function of ILEI during hepatocarcinogenesis. Here, we show that ILEI strictly requires oncogenic Ras to cause TGF-β-independent hepatocellular EMT and tumor progression of hepatocytes. In cooperation with hyperactivated PI3K signaling, exogenous ILEI expression did not affect the epithelial phenotype of hepatocytes, but induced migratory and tumorigenic abilities. ILEI plus oncogenic Ras induced both PDGF-C/PDGF-Rβ expression, which associated with nuclear accumulation of β-catenin and pY-Stat3. Using a dominant-negative PDGF-R mutant, we showed that PDGF-R signaling is causally involved in Ras/ILEI-mediated hepatocellular EMT. Analysis of a human HCC tissue array suggested a correlation between dedifferentiation and poor prognosis with overexpression of cytoplasmically localized ILEI.

Human hepatocarcinogenesis involves ubiquitous, hyperactive Ras signaling as a central event caused by epigenetic silencing of Ras inhibitory proteins (for example, RASSF1A, NORE1A; (Calvisi *et al.*, 2006; Macheiner *et al.*, 2006)). Accordingly, oncogenic Ras and exogenous TGF-β cooperate in normal MIM1-4 hepatocytes to induce and maintain EMT, resulting in an invasive, malignant phenotype, which is associated with autocrine TGF-β signaling (Fischer *et al.*, 2005). This study shows that exogenous ILEI requires co-operation with oncogenic Ras to cause EMT and hepatocellular carcinoma progression in normal MIM1-4 hepatocytes as overexpression of ILEI on its own failed to induce changes in morphology, loss of epithelial markers, migration or tumorigenicity (Supplementary Figures S1a and S2a). In nontumorigenic mammary EpH4 cells, however, ILEI alone was sufficient to induce reversible, density-dependent EMT, tumor growth and lung metastasis after tail vein injection (Waerner *et al.*, 2006). In contrast to the mammary EpH4 model, exogenous ILEI also failed to induce EMT and metastasis in the nontumorigenic MIM-C40 cells, but rendered them migratory and tumorigenic. These results indicate that oncogenic Ras, which causes constitutive hyperactivation of multiple signaling pathways, is strictly required by ILEI to induce EMT and tumor progression in hepatocytes. A possible reason why ILEI plus V12-C40-Ras caused EMT, tumor and metastasis formation in mammary EpC40-ILEI cells could be the fact that these cells show ILEI-enhanced phospho-Erk/MAPK signaling, perhaps cooperating with PI3K hyperactivation to induce EMT. Thus, ILEI probably activates endogenous Ras, since the Ras inhibitor L739.749 abolished EMT in mammary EpC40-ILEI cells (Waerner *et al.*, 2006).

A major difference concerning EMT induction by Ras/ILEI versus Ras/TGF-β in both hepatocytes and mammary cells was that ILEI-induced EMT neither involved nor required autocrine TGF-β secretion. In contrast to mammary cells, MIM1-4-GFP, MIM-C40-GFP and MIM-R-GFP cells secreted TGF-β at rather high levels, which were 2-4-fold reduced by ILEI expression (Supplementary Figure S4). In this line, MIM-C40-GFP and MIM-R-GFP cells showed nuclear localization of Smad2/3, which was partially shifted to a cytoplasmic localization in MIM-C40-ILEI and MIM-R-ILEI cells (Supplementary Figure S3). These cells were also negative for Smad2- and Smad3-dependent activation of luciferase reporter constructs (data not shown). Importantly, the TGF-βRI/II kinase inhibitor LY02109761 failed to revert EMT in MIM-R-ILEI cells (data not shown), suggesting that ILEI-induced EMT of Ras-expressing hepatocytes occurs independently of TGF-β activation, a finding also valid for ILEI-induced EMT in mammary epithelial cells (Waerner *et al.*, 2006).

Recently, we showed that TGF-β/Ras-induced hepatocyte EMT led to activation of PDGF/PDGF-R signaling, which triggers β-catenin to nuclear translocation (Fischer *et al.*, 2007). Here we show that Ras/ILEI-induced EMT involved upregulation of PDGF-C and PDGF-Rβ, whereas epithelial MIM1-4-ILEI and MIM-C40-ILEI cells expressed PDGF-C, but not PDGF-Rβ (Figure 3b). This suggests that an autocrine PDGF-C/PDGF-Rβ loop is important in Ras/ILEI-induced tumor progression, which is supported by the finding that transgenic PDGF-C expression in hepatocytes caused fibrosis and subsequent HCC (Campbell *et al.*, 2005, 2007). Bioactive PDGF-CC ligand showed high-affinity binding to PDGF-Rα/α and PDGF-Rα/β dimers, inducing similar phospho-Erk1/2 levels as PDGF-AB (Pietras *et al.*, 2003). Our idea that ILEI plus Ras-induced autocrine PDGF-C/PDGF-Rβ signaling could activate β-catenin was supported by the finding that a dominant-negative PDGF-Rα mutant (dnP)-inactivating both PDGF-Rα/α and PDGF-Rα/β dimers-was sufficient to reduce nuclear β-catenin levels *in vitro* (data not shown) and *in vivo* (Figure 6). Our observation, however, that dnP could not suppress nuclear β-catenin levels of MIM-R-ILEI tumors down to those observed in MIM-R-GFP-derived tumors, suggests additional mechanisms contributing to nuclear β-catenin activation.

Our finding that Stat3 activation caused by PDGF-R signaling contributes to Ras/ILEI-induced hepatocellular EMT is supported by reports that silencing of the Stat3-inhibitory proteins SOCS1 or SOCS3 by methylation promotes HCC formation by stimulating tumor cell proliferation, survival, migration and angiogenesis (Yoshikawa *et al.*, 2001; Ogata *et al.*, 2006a, b; Yang *et al.*, 2007). Furthermore, activation of Ras and Stat3 by epigenetic inactivation of their endogenous protein inhibitors was ubiquitously detected in human HCC (Calvisi *et al.*, 2006). Thus, the induction of pY-Stat3 by PDGF signaling during Ras/ILEI-induced EMT could be particularly relevant for HCC progression. Whether PDGF-R signaling causes phosphorylation of Stat3 through Jak kinases or Src, the latter shown to act as a Stat3 kinase downstream of PDGF-R signaling (Silva, 2004), remains to be clarified.

In this study, the novel EMT inducer ILEI was shown to cause EMT and tumor progression in normal hepatocytes expressing oncogenic Ras, suggesting that ILEI substitutes for tumor-progressive functions of TGF-β signaling in the liver. As MIM1-4 hepatocytes are more comparable to normal cells than the murine EpH4 or human HMEC mammary epithelial cell models, it was not entirely unexpected that ILEI required oncogenic Ras to cause EMT and metastasis in MIM1-4 cells. Yet, ILEI was sufficient for EMT induction in the EpH4 model through cooperation with chemokine-dependent activation of endogenous Ras. The requirement of Ras/ILEI to cause EMT and tumor progression in hepatocytes, together with a putative intracellular mechanism of ILEI action, renders ILEI comparable to a rapidly growing number of epithelial polarity/vesicle-trafficking regulators in *Drosophila*, which, in cooperation with *Drosophila* Ras, cause lethal, invasive larval tumors (Giebel and Wodarz, 2006).

Materials and methods

Cell culture

MIM-R and MIM-C40 hepatocytes were generated by stable retroviral transmission of MIM1-4 cells with oncogenic v-Ha-Ras or C40-V12-Ras, respectively (Fischer *et al.*, 2005). MIM1-4-GFP, MIM-R-GFP and MIM-C40-GFP cells were obtained by stable retroviral transmission of MIM1-4, MIM-R and MIM-C40 cells with pMSV-GFP, respectively, and subsequent cell sorting. MIM1-4-ILEI, MIM-R-ILEI and MIM-C40-ILEI cells were generated by stable transmission of MIM1-4, MIM-R and MIM-C40 cells, with pMSV harboring bicistronic ILEI and GFP (Waerner *et al.*, 2006), respectively, and subsequent cell sorting. To stably interfere with PDGF signaling, MIM-R-ILEI cells were transmitted with pMSV bicistronically expressing the dn PDGF-receptor α and red fluorescent protein (Fischer *et al.*, 2007), resulting in MIM-R-ILEI-dnP cells. Details about culture conditions of MIM hepatocytes are available as Supplementary Information on the *Oncogene* website.

Western blot analysis

Details are available as Supplementary Information on the *Oncogene* website.

Confocal immunofluorescence microscopy

Cells were fixed and permeabilized as described earlier (Gotzmann *et al.*, 2006). Primary antibodies were used at following dilutions: anti-β-catenin (BD Transduction Laboratories (TL), Lexington, UK), 1:100; anti-active-β-catenin (Upstate, Lake Placid, NY, USA), 1:100; anti-E-cadherin (TL), 1:100; anti-α-SMA (Dako, Carpinteria, CA, USA), 1:100; anti-Smad2/3 (TL), 1:100; anti-ZO-1 (Zymed, San Francisco, CA, USA), 1:100; phalloidin (Molecular Probes, Eugene, OR, USA), 1:40. Nuclei were visualized using To-PRO3 (Invitrogen, Carlsbad, CA, USA) or DAPI (Roche, Basel, Switzerland) at dilutions of 1:10 000 and 1:1000, respectively.

Tumor formation *in vivo*

In total, 1×10^6 cells in 50 μl Ringer solution were either orthotopically transplanted into the liver by injection into the spleen or subcutaneously injected into immunodeficient CB-17 SCID mice as described (Mikula *et al.*, 2004; Fischer *et al.*, 2007). Tumor volume and weight were determined after subcutaneous tumor formation as described recently (Fischer *et al.*, 2007). Tumor incidences were equal to 100%, that is, all injected malignant hepatocytes gave rise to experimental tumors. All experiments were performed twice using three mice per cell type and carried out according to the Austrian guidelines for animal care and protection.

Immunohistochemistry

Paraffin-embedded sections of tumor tissues were stained with the following antibodies: anti-β-catenin (TL), 1:100; anti-active β-catenin (Upstate), 1:100; anti-Stat3 (Cell Signaling, Beverly, MA, USA), 1:100; anti-phospho-Stat3 (Cell Signaling), 1:100; anti-E-cadherin (TL), 1:100; anti-ILEI (Waerner *et al.*, 2006), 1:100. More details are available as Supplementary Information on the *Oncogene* website.

Reverse transcriptase PCR (RT–PCR)

Extraction of poly(A)$^+$-mRNA and cDNA synthesis were performed as described recently (Gotzmann *et al.*, 2006). The PCR amplification products were analysed by agarose gel electrophoresis. Details about primer sequences are available as Supplementary Information on the *Oncogene* website.

Proliferation kinetics

In total, 1×10^5 cells were seeded in triplicate and the number of cells in the corresponding cell populations was determined periodically in a multichannel cell analyser (CASY; Schärfe Systems, Reutlingen, Germany). Cumulative cell numbers were generated from the absolute cell counts and their calculated dilution factors (Gotzmann *et al.*, 2002).

Transwell assay

Details are available as Supplementary Information on the *Oncogene* website.

Tissue array

Tissue array (ORIDIS Biomed, Graz, Austria) contained paraffin-embedded specimens of tumors and adjacent normal tissue collected from 69 female and male HCC patients, which were surgically removed between 1995 and 2004. Protocols of the retrospective analyses were approved by the local institutional review board of the Medical University of Graz. All histological specimens were reviewed for histological type and grade. Core biopsies with diameter of 0.6mm were taken from each donor paraffin block. Sections of each tumor, of thickness 4 μm, and adjacent tissue were arrayed in triplicate. After antigen retrieval in sodium-citrate buffer (pH 6.0), the anti-ILEI antibody (Waerner *et al.*, 2006) was used at a dilution of 1:300. More details are available as Supplementary Information on the *Oncogene* website.

Supplementary Material

Refer to Web version on PubMed Central for supplementary material.

Europe PMC Funders Author Manuscripts

Acknowledgments

We thank ORIDIS Biomed for providing HCC tissue arrays and immunohistochemical staining. This work was supported by grants from the Austrian Science Fund, FWF, Grant number SFB F28 and P19598-B13.

References

Breuhahn K, Longerich T, Schirmacher P. Dysregulation of growth factor signaling in human hepatocellular carcinoma. Oncogene. 2006; 25:3787–3800. [PubMed: 16799620]

Bruix J, Boix L, Sala M, Llovet JM. Focus on hepatocellular carcinoma. Cancer Cell. 2004; 5:215–219. [PubMed: 15050913]

Calvisi DF, Ladu S, Gorden A, Farina M, Conner EA, Lee JS, et al. Ubiquitous activation of Ras and Jak/Stat pathways in human HCC. Gastroenterology. 2006; 130:1117–1128. [PubMed: 16618406]

Campbell JS, Hughes SD, Gilbertson DG, Palmer TE, Holdren MS, Haran AC, et al. Platelet-derived growth factor C induces liver fibrosis, steatosis, and hepatocellular carcinoma. Proc Natl Acad Sci USA. 2005; 102:3389–3394. [PubMed: 15728360]

Campbell JS, Johnson MM, Bauer RL, Hudkins KL, Gilbertson DG, Riehle KJ, et al. Targeting stromal cells for the treatment of platelet-derived growth factor C-induced hepatocellular carcinogenesis. Differentiation. 2007; 75:843–852. [PubMed: 17999742]

Edmondson HA, Steiner PE. Primary carcinoma of the liver: a study of 100 cases among 48,900 necropsies. Cancer. 1954; 7:462–503. [PubMed: 13160935]

Eger A, Aigner K, Sonderegger S, Dampier B, Oehler S, Schreiber M, et al. DeltaEF1 is a transcriptional repressor of E-cadherin and regulates epithelial plasticity in breast cancer cells. Oncogene. 2005; 24:2375–2385. [PubMed: 15674322]

El-Serag HB, Rudolph KL. Hepatocellular carcinoma: epidemiology and molecular carcinogenesis. Gastroenterology. 2007; 132:2557–2776. [PubMed: 17570226]

Fischer AN, Fuchs E, Mikula M, Huber H, Beug H, Mikulits W. PDGF essentially links TGF-beta signaling to nuclear beta-catenin accumulation in hepatocellular carcinoma progression. Oncogene. 2007; 26:3395–3405. [PubMed: 17130832]

Fischer AN, Herrera B, Mikula M, Proell V, Fuchs E, Gotzmann J, et al. Integration of Ras subeffector signaling in TGF-{beta} mediated late stage hepatocarcinogenesis. Carcinogenesis. 2005; 26:931–942. [PubMed: 15705598]

Garcia R, Bowman TL, Niu G, Yu H, Minton S, Muro-Cacho CA, et al. Constitutive activation of Stat3 by the Src and JAK tyrosine kinases participates in growth regulation of human breast carcinoma cells. Oncogene. 2001; 20:2499–2513. [PubMed: 11420660]

Giannelli G, Bergamini C, Fransvea E, Sgarra C, Antonaci S. Laminin-5 with transforming growth factor-beta1 induces epithelial to mesenchymal transition in hepatocellular carcinoma. Gastroenterology. 2005; 129:1375–1383. [PubMed: 16285938]

Giebel B, Wodarz A. Tumor suppressors: control of signaling by endocytosis. Curr Biol. 2006; 16:R91–R92. [PubMed: 16461271]

Gotzmann J, Fischer AN, Zojer M, Mikula M, Proell V, Huber H, et al. A crucial function of PDGF in TGF-beta-mediated cancer progression of hepatocytes. Oncogene. 2006; 25:3170–3185. [PubMed: 16607286]

Gotzmann J, Huber H, Thallinger C, Wolschek M, Jansen B, Schulte-Hermann R, et al. Hepatocytes convert to a fibroblastoid phenotype through the cooperation of TGF-beta1 and Ha-Ras: steps towards invasiveness. J Cell Sci. 2002; 115:1189–1202. [PubMed: 11884518]

Grunert S, Jechlinger M, Beug H. Diverse cellular and molecular mechanisms contribute to epithelial plasticity and metastasis. Nat Rev Mol Cell Biol. 2003; 4:657–665. [PubMed: 12923528]

Herath NI, Leggett BA, MacDonald GA. Review of genetic and epigenetic alterations in hepatocarcinogenesis. J Gastroenterol Hepatol. 2006; 21:15–21. [PubMed: 16706806]

Huber MA, Kraut N, Beug H. Molecular requirements for epithelial-mesenchymal transition during tumor progression. Curr Opin Cell Biol. 2005; 17:548–558. [PubMed: 16098727]

Hugo H, Ackland ML, Blick T, Lawrence MG, Clements JA, Williams ED, et al. Epithelial-mesenchymal and mesenchymal-epithelial transitions in carcinoma progression. J Cell Physiol. 2007; 213:374–383. [PubMed: 17680632]

Jechlinger M, Sommer A, Moriggl R, Seither P, Kraut N, Capodiecci P, et al. Autocrine PDGFR signaling promotes mammary cancer metastasis. J Clin Invest. 2006; 116:1561–1570. [PubMed: 16741576]

Kensler TW, Qian GS, Chen JG, Groopman JD. Translational strategies for cancer prevention in liver. Nat Rev Cancer. 2003; 3:321–329. [PubMed: 12724730]

Kondoh N, Wakatsuki T, Hada A, Shuda M, Tanaka K, Arai M, et al. Genetic and epigenetic events in human hepatocarcinogenesis. Int J Oncol. 2001; 18:1271–1278. [PubMed: 11351262]

Lacher MD, Tiirikainen MI, Saunier EF, Christian C, Anders M, Oft M, et al. Transforming growth factor-beta receptor inhibition enhances adenoviral infectability of carcinoma cells via up-regulation of Coxsackie and Adenovirus Receptor in conjunction with reversal of epithelial-mesenchymal transition. Cancer Res. 2006; 66:1648–1657. [PubMed: 16452224]

Lee HC, Kim M, Wands JR. Wnt/Frizzled signaling in hepatocellular carcinoma. Front Biosci. 2006a; 11:1901–1915. [PubMed: 16368566]

Lee TK, Man K, Poon RT, Lo CM, Yuen AP, Ng IO, et al. Signal transducers and activators of transcription 5b activation enhances hepatocellular carcinoma aggressiveness through induction of epithelial-mesenchymal transition. Cancer Res. 2006b; 66:9948–9956. [PubMed: 17047057]

Macheiner D, Heller G, Kappel S, Bichler C, Stattner S, Ziegler B, et al. NORE1B, a candidate tumor suppressor, is epigenetically silenced in human hepatocellular carcinoma. J Hepatol. 2006; 45:81–89. [PubMed: 16516329]

Mikula M, Fuchs E, Huber H, Beug H, Schulte-Hermann R, Mikulits W. Immortalized p19ARF null hepatocytes restore liver injury and generate hepatic progenitors after transplantation. Hepatology. 2004; 39:628–634. [PubMed: 14999681]

Ogata H, Chinen T, Yoshida T, Kinjyo I, Takaesu G, Shiraishi H, et al. Loss of SOCS3 in the liver promotes fibrosis by enhancing STAT3-mediated TGF-beta1 production. Oncogene. 2006a; 25:2520–2530. [PubMed: 16474852]

Ogata H, Kobayashi T, Chinen T, Takaki H, Sanada T, Minoda Y, et al. Deletion of the SOCS3 gene in liver parenchymal cells promotes hepatitis-induced hepatocarcinogenesis. Gastroenterology. 2006b; 131:179–193. [PubMed: 16831601]

Pardali K, Moustakas A. Actions of TGF-beta as tumor suppressor and pro-metastatic factor in human cancer. Biochim Biophys Acta. 2007; 1775:21–62. [PubMed: 16904831]

Pietras K, Sjoblom T, Rubin K, Heldin CH, Ostman A. PDGF receptors as cancer drug targets. Cancer Cell. 2003; 3:439–443. [PubMed: 12781361]

Rossmanith W, Schulte-Hermann R. Biology of transforming growth factor beta in hepatocarcinogenesis. Microsc Res Tech. 2001; 52:430–436. [PubMed: 11170302]

Silva CM. Role of STATs as downstream signal transducers in Src family kinase-mediated tumorigenesis. Oncogene. 2004; 23:8017–8023. [PubMed: 15489919]

Tannapfel A, Busse C, Weinans L, Benicke M, Katalinic A, Geissler F, et al. INK4a-ARF alterations and $_{p}$53 mutations in hepatocellular carcinomas. Oncogene. 2001; 20:7104–7109. [PubMed: 11704835]

Thiery JP, Sleeman JP. Complex networks orchestrate epithelial-mesenchymal transitions. Nat Rev Mol Cell Biol. 2006; 7:131–142. [PubMed: 16493418]

Thorgeirsson SS, Grisham JW. Molecular pathogenesis of human hepatocellular carcinoma. Nat Genet. 2002; 31:339–346. [PubMed: 12149612]

Waerner T, Alacakaptan M, Tamir I, Oberauer R, Gal A, Brabletz T, et al. ILEI: a cytokine essential for EMT, tumor formation, and late events in metastasis in epithelial cells. Cancer Cell. 2006; 10:227–239. [PubMed: 16959614]

Yang J, Mani SA, Donaher JL, Ramaswamy S, Itzykson RA, Come C, et al. Twist, a master regulator of morphogenesis, plays an essential role in tumor metastasis. Cell. 2004; 117:927–939. [PubMed: 15210113]

Yang SF, Wang SN, Wu CF, Yeh YT, Chai CY, Chunag SC, et al. Altered $_{p}$-STAT3 (tyr705) expression is associated with histological grading and intratumour microvessel density in hepatocellular carcinoma. J Clin Pathol. 2007; 60:642–648. [PubMed: 16901975]

Yoshikawa H, Matsubara K, Qian GS, Jackson P, Groopman JD, Manning JE, et al. SOCS-1, a negative regulator of the JAK/STAT pathway, is silenced by methylation in human hepatocellular carcinoma and shows growth-suppression activity. Nat Genet. 2001; 28:29–35. [PubMed: 11326271]

Zhou L, Rui JA, Wang SB, Chen SG, Qu Q, Chi TY, et al. Outcomes and prognostic factors of cirrhotic patients with hepatocellular carcinoma after radical major hepatectomy. World J Surg. 2007; 31:1782–1787. [PubMed: 17610113]

Europe PMC Funders Author Manuscripts

Europe PMC Funders Author Manuscripts

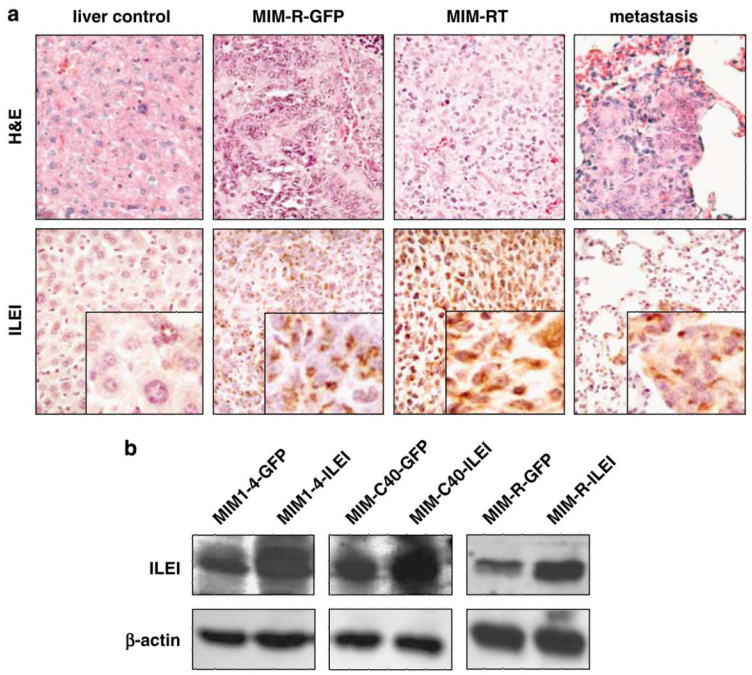

Figure 1.

ILEI expression in moderately or poorly differentiated experimental liver tumors and in ILEI-transduced hepatocytes. Epithelial MIM-R-GFP hepatocytes, or MIM-RT cells that have undergone EMT, were orthotopically transplanted into the spleen or injected by tail vein. Liver tumors were collected after 20 days and processed for histology and immunohistochemistry. (**a**) Sections from wild-type BALB/c livers (control), MIM-R-GFP- and MIM-RT-generated liver tumors and lung metastases induced after tail vein injection of MIM-RT cells were stained with hematoxylin and eosin (H&E) or immunohistochemically stained with anti-ILEI antibody. Insets show staining of tumor sections at 4-fold higher magnification to reveal endogenous ILEI localization. (**b**) ILEI-overexpressing MIM1-4-ILEI, MIM-C40-ILEI and MIM-R-ILEI cells or empty vector expressing MIM1-4-GFP, MIM-C40-GFP and MIM-R-GFP cells were analysed by immunoblotting using anti-ILEI and anti-β-actin antibodies. The expression of β-actin is shown as a loading control. ILEI, interleukin-like EMT inducer.

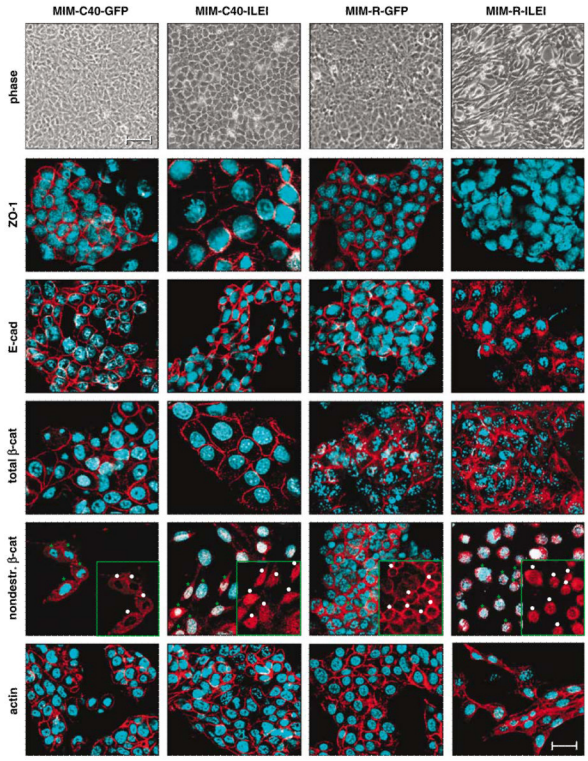

Figure 2.

ILEI causes the disassembly of epithelial junctions, cytoskeletal reorganization and β-catenin activation in cooperation with oncogenic Ras. Phase contrast images of MIM-C40-GFP, MIM-C40-ILEI, MIM-R-GFP and MIM-R-ILEI cells are shown in the top panels (scale bar: 50 μm). The lower panels show confocal immunofluorescence images of these cell types after staining with specific antibodies against ZO-1, E-cadherin (E-cad), total β-catenin (total β-cat), activated, nondestructible β-catenin (nondestr. β-cat) and phalloidin to visualize β-actin. Blue-green staining: DNA. Scale bar in confocal images: 15 μm. Insets (green border): cells marked by white dots are shown without DNA staining to better visualize cytoplasmic versus nuclear staining of activated β-catenin (green asteriks in main panel mark DNA staining). ILEI, interleukin-like EMT inducer.

Europe PMC Funders Author Manuscripts

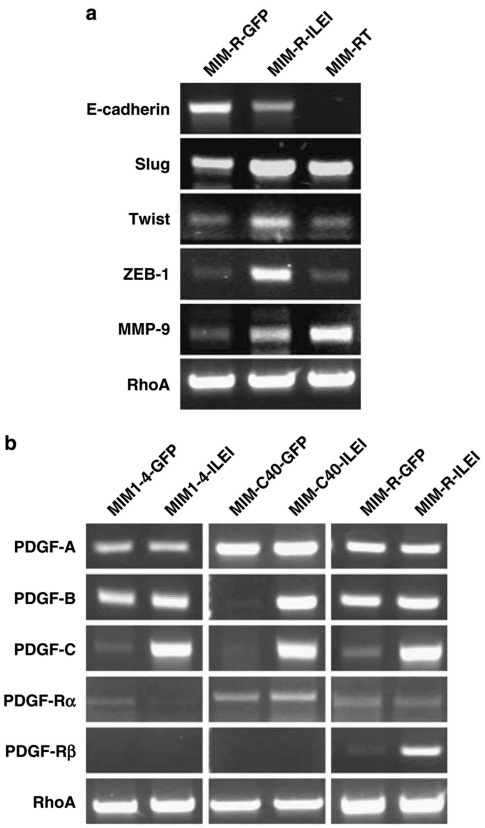

Figure 3.

Expression of EMT markers and PDGF/PDGF-R isoforms in hepatocytes before and after ILEI overexpression. (**a**) Expression levels of transcripts for E-cadherin, the E-cadherin-repressing transcription factors Slug, Twist and ZEB-1, and the matrix metalloproteinase MMP-9 in MIM-R-GFP, MIM-R-ILEI and MIM-RT cells (positive EMT control), as determined by linear semi-quantitative RT–PCR. (**b**) Individual transcript levels of three PDGF isoforms (PDGF-A, -B and -C) and two PDGF-receptor isoforms (PDGF-Rα and PDGF-Rβ) were analysed by linear semi-quantitative RT–PCR in MIM1-4-GFP, MIM1-4-ILEI, MIM-C40-GFP, MIM-C40-ILEI, MIM-R-GFP and MIM-R-ILEI cells. Constitutive levels of RhoA mRNA are shown as a loading control. EMT, epithelial to mesenchymal transition; PDGF, platelet-derived growth factor; RT–PCR, Reverse transcriptase–PCR; ILEI, interleukin-like EMT inducer.

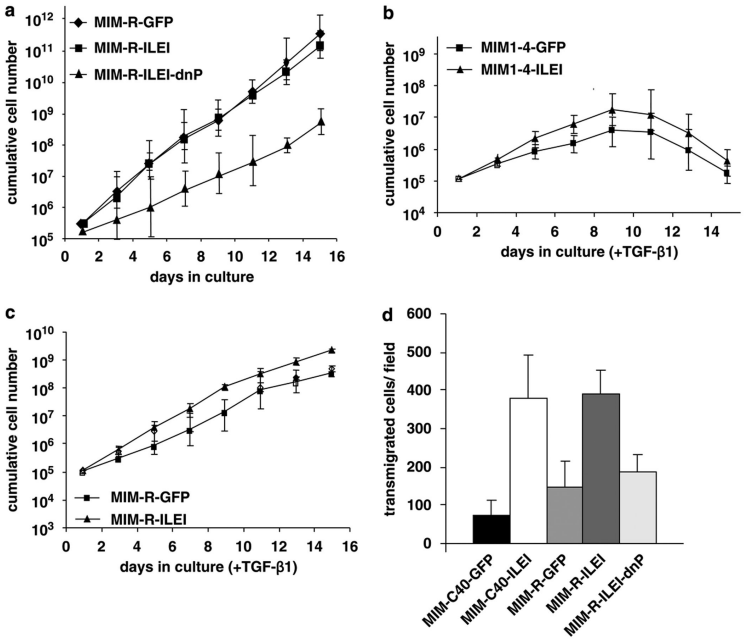

Figure 4.

ILEI modulates migratory behavior of hepatocytes but has little effect on proliferation. (a–c) Proliferation kinetics were determined by cumulative cell numbers. (**a**) Proliferation kinetics of untreated MIM-R-GFP, MIM-R-ILEI and MIM-R-ILEI-dnP cells. (**b**) Proliferation kinetics of MIM1-4-GFP and MIM1-4-ILEI cells as well as (**c**) MIM-R-GFP and MIM-R-ILEI cells during treatment with TGF-β1 (1 ng/ml). (**d**) Control cells (MIM-C40-GFP and MIM-R-GFP), ILEI-overexpressing cells (MIM-C40-ILEI and MIM-R-ILEI) and ILEI-overexpressing MIM-R-GFP cells harboring a dominant-negative PDGF-Rα (MIM-R-ILEI-dnP) after transmigration through Transwell filters. Migrated cells were visualized by Hoechst staining under UV-light and counted (numbers represent transmigrated cell numbers per standard microscopic field). Error bars denote s.e.m. ILEI, interleukin-like EMT inducer.

Europe PMC Funders Author Manuscripts

Europe PMC Funders Author Manuscripts

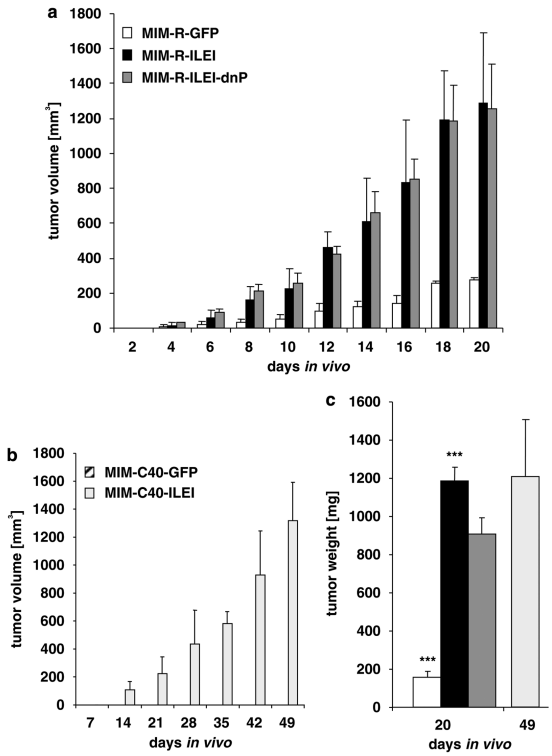

Figure 5.

ILEI enhances tumor formation in synergy with oncogenic Ras and induces tumorigenicity in nontumorigenic hepatocytes expressing the PI3K-hyperactivating Ras mutant V12-C40. Tumors were generated in SCID mice by subcutaneous injection of MIM-R-GFP (**a**, white bars), MIM-R-ILEI-dnP (**a**, dark gray bars), MIM-R-ILEI cells (**a**, black bars) and MIM-C40-ILEI (**b**, light gray bars). Control MIM-C40-GFP hepatocytes (**b**, hatched bars) failed to form tumors. (**a** and **b**) Kinetics of tumor formation as determined by calculation of tumor volumes. (**c**) Weights of tumor tissues collected after 20 days (MIM-R-GFP, white bar; MIM-R-ILEI, black bar; MIM-R-ILEI-dnP, dark gray bar) or 49 days (MIM-C40-ILEI, light gray bar). Statistically significant weight differences ($P<0.0005$) between MIM-R-GFP and MIM-R-ILEI tumors are indicated with ***. (**a–c**) One representative experiment out of three is shown. Error bars denote s.e.m. SCID, severe combined immunodeficiency; ILEI, interleukin-like EMT inducer.

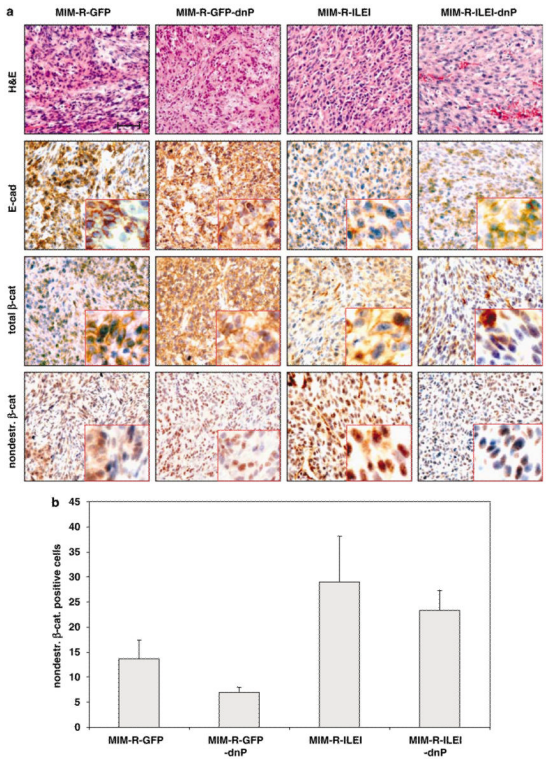

Figure 6.

Ras plus ILEI expression increases nuclear β-catenin levels *in vivo*, which requires PDGF-R signaling. (**a**) Experimental tumors obtained after subcutaneous injection of MIM-R-GFP, MIM-R-GFP-dnP, MIM-R-ILEI or MIM-R-ILEI-dnP cells into SCID mice were collected after 20 days and processed for histology and immunohistochemistry using anti-E-cadherin (E-cad), anti-β-catenin (total β-cat) or anti-activated, nondestructible β-catenin (nondestr. β-cat) antibodies. Bar, 50 μm. Insets show staining of tumor sections at fivefold higher magnification to reveal details of E-cadherin localization at cell membranes and nuclear β-catenin. (**b**) Quantitative evaluation of cells for nuclei expressing activated, nondestructible β-catenin. Error bars depict s.e.m. from three independent experiments. SCID, severe combined immunodeficiency; ILEI, interleukin-like EMT inducer.

Europe PMC Funders Author Manuscripts

Europe PMC Funders Author Manuscripts

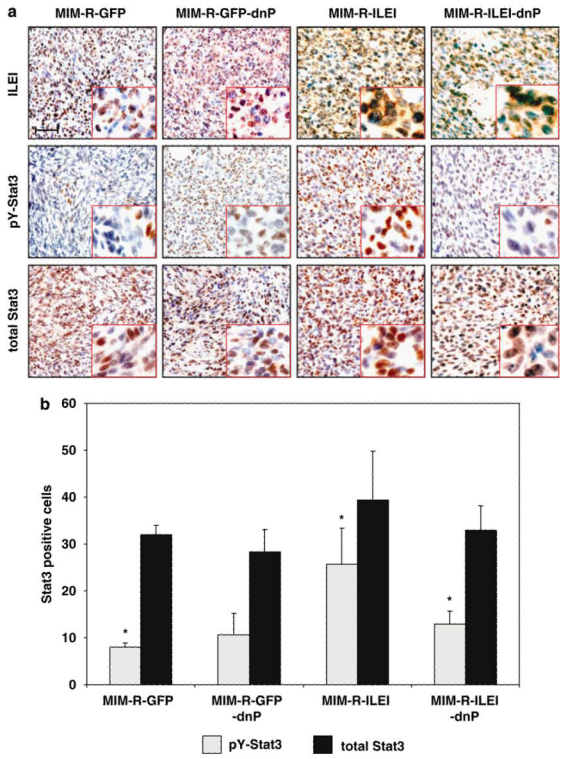

Figure 7.

The cooperation of ILEI and Ras activates Stat3 in a PDGF-dependent fashion. (**a**) Subcutaneous tumors were generated in SCID mice, collected after 20 days and processed for immunohistochemistry, employing anti-ILEI, anti-phospho-Stat3 (pY-Stat3) and anti-total Stat3 (total Stat3) antibodies for staining. Bar: 50 μm. Insets: fivefold enlarged images to reveal details in granular versus cytoplasmic ILEI staining and nuclear pY-Stat3 staining. (**b**) Quantitative evaluation of cell nuclei positive for tyrosine-phosphorylated Stat3 (pY-Stat3; gray bars) and total Stat3 (black bars). Statistically significant differences ($P<0.05$) in expression of pY-Stat3 are indicated with asterisk. SCID, severe combined immunodeficiency; ILEI, interleukin-like EMT inducer; PDGF, platelet-derived growth factor.

Europe PMC Funders Author Manuscripts

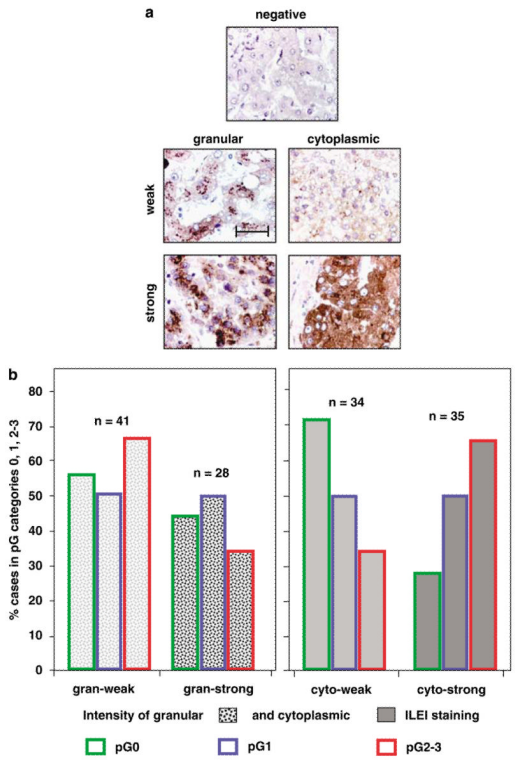

Figure 8.

Intensity and pattern of ILEI expression predicts tumor dedifferentiation and prognosis of human HCCs. A tissue array containing 69 human HCC samples and respective control liver tissues were immunohistochemically stained with anti-ILEI antibody. (**a**) Representative examples shown are for no (negative), weak or strong granular and cytoplasmic ILEI staining of the HCC tissue array. Scale bar: 200 μm. (**b**) The intensity of granular (gran; left panel) and cytoplasmic (cyto; right panel) ILEI staining (weak including negative or strong) was correlated with postoperative histological grading (pG) of the HCC in the array ranging from well-differentiated (pG1) to moderately (pG2) and poorly dedifferentiated HCCs (pG3). pG2 and pG3 were grouped together because of low sample numbers for pG3. Whereas strong granular staining slightly correlated with more differentiated HCC, strong cytoplasmic staining correlated with poorly differentiated HCC and thus bad prognosis. The comparison of the tumor grading distribution between the groups cytoplasmic weak and cytoplasmic strong was significant ($P<0.05$) showing a higher percentage of pG1 and pG2–3 tumors in the group cytoplasmic strong than in group cytoplasmic weak. ILEI, interleukin-like EMT inducer; HCC, hepatocellular carcinoma.